Materials Letters 91 (2013) 121–124

Contents lists available at SciVerse ScienceDirect

Materials Letters

journal homepage: www.elsevier.com/locate/matlet

Development of biporous Ti_3AlC_2 ceramic wicks for loop heat pipe

Jiyuan Xu [a], Yong Zou [b,*], Deshuai Yang [b], Mingxiu Fan [a]

[a] School of Energy and Power Engineering, Shandong University, Jinan 250061, Shandong, China
[b] Key Laboratory of Liquid Structure and Heredity of Materials, Ministry of Education, Shandong University, Jinan 250061, Shandong, China

ARTICLE INFO

Article history:
Received 19 July 2012
Accepted 20 September 2012
Available online 29 September 2012

Keywords:
Ti_3AlC_2
Loop heat pipe
Porous materials
Ceramics

ABSTRACT

Novel Ti_3AlC_2 wicks with two distinguished characteristic pore sizes were successfully developed. The heat transfer performances of the loop heat pipes with monoporous and biporous Ti_3AlC_2 wicks were comparatively studied. Results show that Ti_3AlC_2 wicks exhibit increased porosity and reduced thermal conductivity by using salt leaching pore-forming and two kinds of pores can be found in one Ti_3AlC_2 wick. Moreover, the loop heat pipe with biporous Ti_3AlC_2 wick operates reliably under the heat load of 25 W compared with that employing monoporous Ti_3AlC_2 wick. Biporous Ti_3AlC_2 wicks proved to be possible alternatives to metals and conventional ceramics for applications in LHP wicks.

1. Introduction

Loop heat pipe (LHP) has been extensively used in thermal management fields with a porous wick in its evaporator to provide high capillary force to circulate the fluid [1,2]. In order to guarantee the stability of LHP systems, researchers aim at developing wicks which can simultaneously provide high capillary force, permeability and low thermal conductivity. In a wick, small pores should be employed for high capillary suction [1], but on the other hand, small pores will trap vapor and prevent rewetting. It indicates that the wicks with single pore characterization exhibit poor compromise between high capillary force and high vapor permeability. In aspect of materials selection, sintered metals such as nickel and copper have been widely used due to their good pore-forming abilities. However, heat leak through the wicks becomes serious due to their high thermal conductivities [3]. Ceramic wicks with lower thermal conductivity have attracted great interest [2], however, most conventional ceramics present brittleness, low pore-forming ability and thermal shock resistance. Therefore, it is desirable to develop novel ceramic wicks which can meet with several constraints (e.g. good machinability, high mechanical strength, thermal shock resistance, etc.) simultaneously.

In recent years, the $M_{n+1}AX_n$ phases (where M represents early transition elements, A is an A group element, X is C or N, and $n=1$, 2, 3) (e.g. Ti_2AlC and Ti_3AlC_2) have attracted increased interest due to their superior properties, such as good machinability, high mechanical strength, thermal shock resistance and excellent oxidation, corrosion resistance, etc. [4,5], which provide exciting opportunities for applications in two-phase heat transfer fields. Lots of efforts have been made for synthesizing dense $M_{n+1}AX_n$ materials [6–8]. However, a little research has been carried out on their applications [5], especially on porous $M_{n+1}AX_n$ phases. Up to now, no relevant report about $M_{n+1}AX_n$ phase wick for LHP has been found.

In this study, cold-pressing sintering coupled with pore-forming was employed to fabricate porous Ti_3AlC_2, and the pore characteristics were studied. Two kinds of Ti_3AlC_2 wicks with different pore structures were employed in LHPs and the heat transfer performances were comparatively studied.

2. Experimental

Fabrication: Ti (-40 μm, 99.9%), TiC (-10 μm, 99%) and Al (-10 μm, 99.9%) were weighted in the stoichiometric ratio of Ti:TiC:Al$=$1:2:1.1, with Al slightly off-stoichiometric to compensate the oxidized Al at high temperatures. NaCl (400 mesh, 99.9%) was used as a pore former. The powders were fully mixed and further refined for 60 min by ball milling and then transferred into a closed graphite mold and cold pressed at 5 MPa. After that the mold with mixed powders was sintered in argon atmosphere at 1300 °C for 120 min. The heating rate was 25 °C/min. Finally, the sintered products were kept in a constant temperature water bath at 90 °C for 3 h to dissolve NaCl. Deionized water was employed as a solvent and ultrasonic cleaning machine was used to accelerate the dissolution process.

Characterization: The phase composition was determined using an X-ray diffractometer (XRD; Cu Kα radiation). The scanning rate and scanning step were fixed at 4°/min and 0.02°, respectively. Surface morphology was observed by scanning electron microscopy (SEM; JSM-6610LV, Japan). The porosity of the wicks was

* Corresponding author. Tel./fax: +86 531 88399872.
E-mail address: yzou@sdu.edu.cn (Y. Zou).

0167-577X/$ - see front matter
http://dx.doi.org/10.1016/j.matlet.2012.09.083

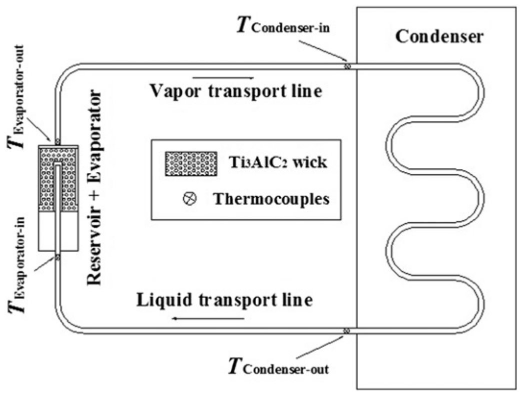

Fig. 1. Scheme of LHP experiment.

determined according to Archimedes' displacement method [3]. The thermal conductivity was measured using Hot Disk TPS 2500 S, with the reproducibility typically better than 1% and the accuracy better than 5% [9].

The performance tests were carried out on LHPs with two different wicks using deionized water as the working fluid at 25 W. Fig. 1 shows the LHP in which the evaporator has 40 mm length and 17 mm inner diameter, the reservoir has the same diameter as the evaporator and a length of 25 mm, the transport lines of liquid (length of 350 mm) and vapor (length of 320 mm) have 2 mm inner diameter. The condenser (length of 800 mm) was cooled by a heat sink at 20 °C. The inlet and outlet temperatures of evaporator and condenser were measured using type-T thermocouples.

3. Results and discussion

Phase composition and microstructure: The author elucidated the synthesis mechanism of Ti_3AlC_2 in the previous study [10],

$$4Ti+2Al=TiAl+Ti_3Al \tag{1}$$

$$Ti_3Al+2Al=3TiAl \tag{2}$$

$$TiAl+TiC=Ti_2AlC \text{ (211 family)} \tag{3}$$

$$Ti_2AlC+TiC=Ti_3AlC_2 \text{ (312 family)} \tag{4}$$

Fig. 2(a) shows the XRD result of sintered product after dissolving NaCl. The major phase is Ti_3AlC_2, with a little Ti_2AlC, TiC and unreacted Ti. Peaks of chloride are not detected. In other words, the dominating reaction was synthesizing Ti_3AlC_2 while NaCl did not react with the original mixture.

Although the sintering temperature obviously exceeded the melting point of NaCl, the strictly sealed graphite mold prevented melted NaCl spilling over. Fig. 2(b) and (c) shows the SEM images of the wicks at low magnification with 0% and 30% NaCl, respectively. Compared with Fig. 2(b), it is obviously observed in Fig. 2(c) that a great number of large pores with pore size ranging from 15 μm to 50 μm are uniformly distributed in the sample after dissolving NaCl. Both the morphology and the size of pores are quite in agreement with the sieved NaCl powders (as shown in the inset image of Fig. 2(c)), indicating that these large pores are formed due to the occupation of NaCl powders. Detailed result is shown in Fig. 2(d), which is high-magnification observation of Fig. 2(c). In addition to large pores existing in one sample, fine pores (< 5 μm) between the grains (with the average

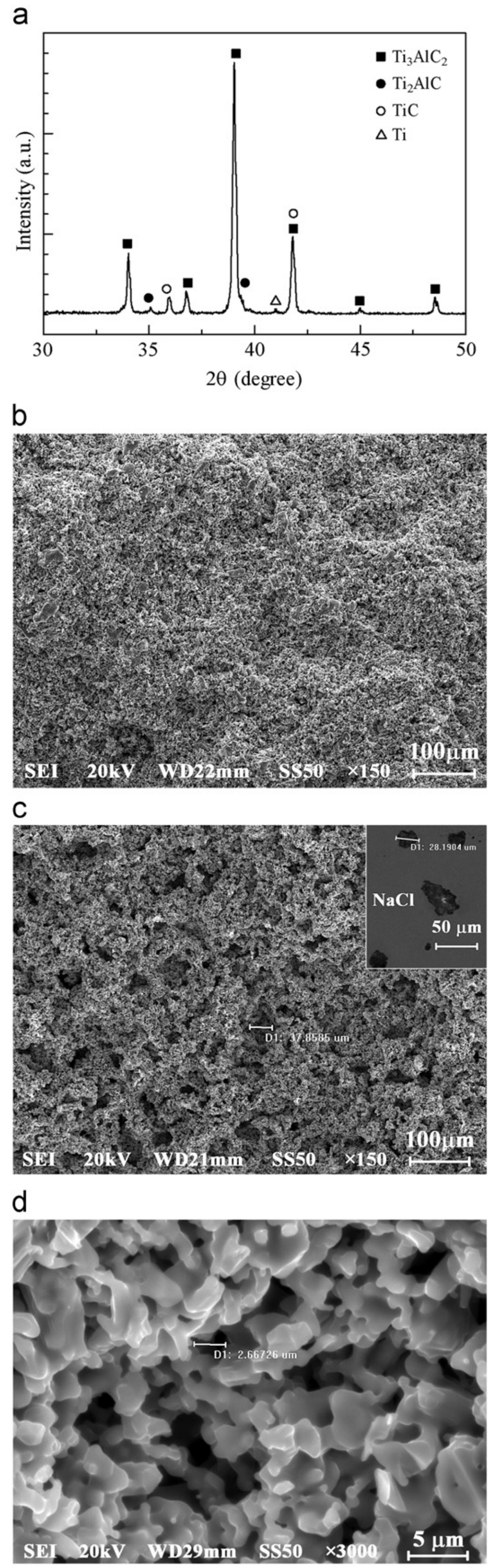

Fig. 2. (a) XRD pattern of Ti_3AlC_2 after dissolving NaCl; (b, c) are low-magnification observations of Ti_3AlC_2 wick without NaCl and with 30% NaCl, respectively. The inset image of (c) shows the morphology of 400 mesh NaCl and (d) high-magnification observation of Ti_3AlC_2 wicks with 30% NaCl.